

Title page

**Daily soil temperature modeling improved by integrating observed snow cover and estimated soil moisture in the U.S. Great Plains**

H. Zhao<sup>1</sup>, G. F. Sassenrath<sup>2,3</sup>, M. B. Kirkham<sup>3</sup>, N. Wan<sup>1</sup>, X. Lin<sup>1\*</sup>

5

<sup>1</sup>Department of Agronomy, Kansas Climate Center, Kansas State University, Manhattan, KS, USA

<sup>2</sup>Southeast Research and Extension Center, Parsons, KS, USA

<sup>3</sup>Department of Agronomy, Kansas State University, Manhattan, KS, USA

10 *Correspondence to:* X. Lin ([xlin@ksu.edu](mailto:xlin@ksu.edu))

## Abstract

15 Soil temperature ( $T_s$ ) plays a critical role in land-surface hydrological processes and agricultural ecosystems. However, soil temperature data are limited in both temporal and spatial scales due to the configuration of early weather station networks in the U.S. Great Plains. Here, we examined an empirical model (EM02) for predicting daily soil temperature ( $T_s$ ) at the 10 cm depth across Nebraska, Kansas, Oklahoma, and parts of Texas that comprise the U.S. winter wheat belt. An improved empirical  
20 model (iEM02) was developed and calibrated using available historical climate data prior to 2015 from 87 weather stations. The calibrated models were then evaluated independently using the latest 5-year observations from 2015 to 2019. Our results suggested that the iEM02 had, on average, an improved root mean square error (RMSE) of 0.6°C for 87 stations when compared to the original EM02 model. Specifically, after incorporating changes in soil moisture and daily snow depth, the improved model  
25 was 50% more accurate as demonstrated by the decrease in RMSE. We conclude that in the U.S. Great Plains the iEM02 model can better estimate soil temperature at the surface soil layer where most hydrological and biological processes occur. Both seasonal and spatial improvements made in the improved model suggest that it can provide a daily soil temperature modeling tool that overcomes the deficiencies of soil temperature data used in assessments of climatic changes, hydrological modeling,  
30 and winter wheat production in the U.S. Great Plains.

## 1 Introduction

A reliable estimate of soil temperature ( $T_s$ ) is useful to understand agricultural ecological systems, hydrological processes, and land-atmosphere interactions (Lembrechts et al., 2020; Qi et al., 2016; Zhang et al., 2018) due to the fact that  $T_s$  governs physical, chemical, and biological processes of the soil and interactions between the atmosphere and land-surface (Smith, 2000; Soong et al., 2020). In particular,  $T_s$  has been widely used for a better understanding of changes in soil moisture (Lakshmi et al., 2003), the ecosystem carbon balance (Goulden et al., 1998), and the nitrogen mineralization process (Persson and Wirén, 1995) although a larger prevalence of air temperature observations are available as a soil temperature proxy. From a practical perspective,  $T_s$  is critical for agricultural system models such as the crop environmental resource synthesis (CERES) models to assess the impacts of extreme climate on crop production and stress tolerance, thereby allowing producers to better prepare for proactive and reactive field management (Bergjord et al., 2008; Persson et al., 2017; Williams et al., 1989). Frequent extreme climate events such as spring freezes and summer heat stress can impact winter wheat [*Triticum aestivum* L.] growth and development, reducing grain yields by more than 7% in the U.S. winter wheat belt (Tack et al., 2015; Paulsen and Heyne, 1983). These effects are also modulated through land-surface interaction processes (Hillel, 1998; Araghi et al., 2017).

To improve the accuracy of crop management modeling, a bare soil temperature ( $T_s$ ) at the 10 cm depth, a standard soil temperature variable, has commonly been considered as a more direct and useful variable than air temperature ( $T_a$ ) measured at 1.5 or 2 m height in crop phenology (Onwuka and Mang, 2018), plant photosynthesis and soil respiration (Meyer et al., 2018; Wu and Jansson, 2013), plant

nutrient uptake (Yan et al., 2012), and estimate of crop production (Araghi et al., 2017; Hillel, 1998). There are many  $T_s$  modeling techniques mostly based on the land-surface interaction process (Qi et al., 2019; Yener et al., 2017). Most  $T_s$  models are rooted in theories of soil heat exchange and surface energy balance (Rankinen et al., 2004; Nobel and Geller, 1987; Chalhoub et al., 2017). The theory-based simulation for surface energy balance usually includes solar radiation (incoming and outgoing), infrared radiation (absorbed and reflected), turbulent flux energy (latent heat and sensible heat), and net ground heat flux through the ground surface into soil layers thermodynamically (Mihalakakou et al., 1997; Chalhoub et al., 2017). Obviously, the energy-balance based model usually requires more detailed near-surface and soil variables such as turbulent flux quantities (sensible heat flux and latent heat flux) to make the model reliable and accurate; however, determining quality turbulent flux quantities is not a trivial task (Dhungel et al., 2021; Kutikoff et al., 2021). In addition, seasonal variations of soil thermal conductivity and underestimates of actual evapotranspiration usually lead to overestimated surface soil temperatures (Bittelli et al., 2008). Therefore, simpler empirical models with fewer dynamic processes for  $T_s$  prediction have been explored (Zheng et al., 1993; Plauborg, 2002; Liang et al., 2014; Badache et al., 2016; Kang et al., 2000). However, these empirical models might result in relatively large estimated errors of over 2°C due to the lack of details about physical process such as uncertainties of the soil volumetric heat capacity and thermal conductivity (Badía et al., 2017). For example, the volumetric heat capacity was higher for a clay soil (1.48 ~3.54 MJ m<sup>-3</sup> °C<sup>-1</sup>) than for a sand soil (1.09 ~ 3.04 MJ m<sup>-3</sup> °C<sup>-1</sup>) when the soil moisture content was between 0 to 0.25 kg kg<sup>-1</sup> (Abu-Hamdeh, 2003). Currently, the U.S. Department of Agriculture (USDA) provides a high-resolution Gridded Soil Survey Geographic (gSSURGO) Database product (<https://gdg.sc.egov.usda.gov/>) that includes static soil physical property

data at 10 km resolution (USDA NRCS, 2013). The gSSURGO data facilitate  $T_s$  modeling, especially for better performance in large-scale  $T_s$  modeling due to its spatial variations in soil properties and soil moisture (USDA NRCS, 2013). These datasets have been widely used in the estimation of root-zone soil water content (Miller et al., 2018) and sub-surface hydrologic properties (Dirmeyer and Norton, 2018). The empirical model proposed by Plauborg (2002) performed better than energy-balance based models when applied in the U.S. Great Plains for the last five years. Due to the lack of information about static soil properties on a large scale one or two decades ago, either over- or underestimates of  $T_s$  occurred, which in turn leads to large deviations in the assessment of crop stress and crop production (Gupta et al., 1990; Stone et al., 1999).

Recent studies have shown that estimated soil temperature usually deviates from observed soil temperature in the winter due to snow cover, frozen soil, and wide spatial and temporal heterogeneity in frozen soil properties (Nagare et al., 2012; Zhang et al., 2008; Rankinen et al., 2004). The impact of snow cover on soil temperature has been investigated (Rankinen et al., 2004) and is partially accounted for by incorporating correcting factors in land-surface modeling as well as ecosystem models (Zhang et al., 2008) and soil and water assessment tools (SWAT) (Qi et al., 2019). For both empirically and physically-based soil temperature modules embedded in SWAT, the predictions of soil temperature in regions with thick snow cover seldom agree with field measurements in winter (Qi et al., 2019).

In the U.S. Great Plains, there has been increasing interest in improving hydrological process modeling of surface water and groundwater due to the Ogallala aquifer's depletion in recent decades (Haacker et al., 2019). However, the automated weather station networks that observed soil temperature were not

commissioned in this region until the late 1980s and early 1990s (Brock and Crawford, 1995). Not only  
95 were there few continuous observations for  $T_s$  earlier than the 1990s, these automated weather station  
networks also had limited stations in each state of the U.S. Great Plains. Such a lack of reliable soil  
temperature data both spatially and temporally makes the long-term assessment of water resources, crop  
phenology, and crop production modeling difficult.

100 The objectives of this study include: (1) develop a robust  $T_s$  model using limited surface climate  
variables by integrating soil moisture as well as snow depth observations; (2) demonstrate the error  
contributions in soil temperature modeling; and (3) evaluate the performance of an improved model to  
predict  $T_s$  compared to current models. The datasets and methods are described in section 2. Section 3  
provides modeling results and conclusions are presented in section 4.

105

## **2 Datasets and Methods**

### **2.1 Weather stations and datasets**

The spatial domain of this study covers the winter wheat belt in the U.S. Great Plains, comprising the  
states of Nebraska (NE), Kansas (KS), Oklahoma (OK), and part of Texas (TX) where soil texture and  
110 bulk density vary (Fig. 1). In this study, three surface climate datasets were obtained from: (1) the  
Automated Weather Data Networks (AWDN) (<https://hprcc.unl.edu/awdn/>), commissioned in the 1980s  
for Nebraska and Kansas; (2) the Oklahoma Mesonet is a daily climate data source for Oklahoma,  
which started in the 1990s (<http://www.mesonet.org/>); and (3) the Soil and Climate Analysis Network,  
which gives daily climate observations (<https://www.wcc.nrcs.usda.gov/scan/>) that we selected for

115 Texas due to limited quality data available in its automated weather station network. The number of  
selected stations was 26 in NE, 8 in KS, 44 in OK, and 9 in TX. The selection of these 87 stations was  
based on the completeness of climate data and data length (at least longer than a continuous 15-year  
periods). In addition to the weather station datasets, soil datasets providing soil attributes and  
characteristics were obtained from the standard USDA-NRCS Soil Survey Geographic (gSSURGO)  
120 Database product (<https://gdg.sc.egov.usda.gov/>), from which soil bulk density ( $\rho_b$ , g cm<sup>-3</sup>), soil organic  
matter ( $f_{OM}$ , %), sand ( $f_{sa}$ , %), clay ( $f_{cl}$ , %), silt ( $f_{sl}$ , %) contents, soil porosity ( $\emptyset$ , %), and soil surface  
albedo ( $\alpha$ , -) were used for all weather stations. Note that all symbols and corresponding descriptions  
for variables used in this study are listed in the Table A1 (see the Appendix). The snow depth data were  
taken from the daily Global Historical Climatology Network (GHCN) (Menne et al., 2009; Lin et al.,  
125 2017). Detailed dataset sources and data variables used in each dataset are shown in Table A2 (see the  
Appendix).

## 2.2 Soil temperature models

### 2.2.1 Empirical model

130 There are two common soil temperature models: empirical and process-based. After examining both  
types of models for our study region, the current empirical model was selected because it was more  
accurate than the process-based model in this area. Plauborg (2002) developed a statistical soil  
temperature ( $T_s$ , °C) model based on the current and previous two-day air temperatures ( $T_a$ , °C), annual  
and semi-annual cycles in the soil temperature fluctuations, and a daily soil temperature offset at a  
135 specific site, as shown in Eq. (1) (called EM02, thereafter):

$$T_{s,j} = \gamma + \alpha_0 T_{a,j} + \alpha_1 T_{a,j-1} + \alpha_2 T_{a,j-2} + \beta_1 \sin(\omega j) + \delta_1 \cos(\omega j) + \beta_2 \sin(2\omega j) + \delta_2 \cos(2\omega j) \quad (1)$$

where  $\gamma$  is an offset constant ( $^{\circ}\text{C}$ ) and coefficients  $\alpha_0$ ,  $\alpha_1$ , and  $\alpha_2$  are dimensionless. The units of the coefficients  $\beta_1$ ,  $\beta_2$ ,  $\delta_1$ , and  $\delta_2$  are Celsius ( $^{\circ}\text{C}$ ). The  $j$  and  $\omega$  denote day of the year and annual frequency (140  $(2\pi/365$  or  $2\pi/366$  in leap years) in an annual soil temperature signal.

### 2.2.2 Improved empirical model

The improved model, based on the EM02, was developed through the following three steps: (1) prolonging the time window of  $T_a$  to include one extra prior day  $T_a$ ; (2) constructing a new fictive (145 environmental temperature ( $T_{env}$ ,  $^{\circ}\text{C}$ ) defined as a function of air temperature and surface skin temperature ( $T_{sfc}$ ,  $^{\circ}\text{C}$ ) (Williams et al., 1984) utilizing  $T_{env}$  to replace the original  $T_a$ ; and most importantly (3), incorporating site-specific daily soil thermal diffusivity and snow depth. This improved empirical model (iEM02) can be described by Eqs. (2-6):

$$T_{s,j} = (\gamma + \alpha_0 T_{env,j} + \alpha_1 T_{env,j-1} + \alpha_2 T_{env,j-2} + \alpha_3 T_{env,j-3} + \beta_1 \sin(\omega j) + \delta_1 \cos(\omega j) + \beta_2 \sin(2\omega j) + \delta_2 \cos(2\omega j)) \times f(D_{s,j}) \times DR_{eff,j} \quad (2)$$

$$T_{env,j} = \beta T_{a,j} + (1 - \beta) T_{sfc,j} \quad (3)$$

$$T_{sfc,j} = (1 - \alpha) \left( \bar{T}_{a,j} + (\bar{T}_{max,j} - \bar{T}_{a,j}) \sqrt{\frac{R_{s,j}}{33.5}} \right) + \alpha T_{sfc,j-1} \quad (4)$$

$$f(D_{s,j}) = \exp(-f_s D_{s,j}) \quad (5)$$

$$DR_{eff,j} = \exp\left(k_0 \sqrt{-h \frac{\pi}{k_{s,j} p}}\right) \quad (6)$$



155 where a fictive environmental temperature ( $T_{env}$ ) is assumed to be the weighted mean of air temperature ( $T_a$ ) at 2 m and surface temperature ( $T_{sfc}$ ). The  $\beta$  refers to the weighting coefficient, which defines the relative weight of the air temperature. This weighted fictive temperature will help weigh surface cooling and heating due to radiative and convective process (Dolschak et al., 2015). The  $T_{sfc}$  in Eq. (3) was estimated iteratively from the three-day running average of daily air temperature ( $\bar{T}_a$ ), daily maximum  
160 temperature ( $\bar{T}_{max}$ , °C), and daily solar radiation ( $R_s$ , MJ m<sup>-2</sup> d<sup>-1</sup>). The  $\alpha$  denotes soil surface albedo (-) and initial  $T_{sfc,j-1}$  was set as annual mean  $T_a$  in Eq. (4). The constant 33.5 is an empirical constant (MJ m<sup>-2</sup> d<sup>-1</sup>) (Williams et al., 1984). The function of snow cover on the j<sup>th</sup> day is given as  $f(D_{S,j})$  and was introduced based on the work of Rankinen et al., (2004). The  $f_s$  and  $D_S$  are empirical soil heat damping parameters (m<sup>-1</sup>) and snow depth (m). The damping ratio of soil at the soil depth of  $h$  ( $h = 0.1$  m in this  
165 study) is  $DR_{eff,j}$  (Rosenberg et al., 1983). The weighting coefficient for the damping ratio (-) is  $k_0$ . The  $p$  represents the period (365 days or 366 days in a leap year) in an annual cycle. The thermal diffusivity  $k_{s,j}$  (m<sup>2</sup> s<sup>-1</sup>) is equivalent to thermal conductivity ( $\lambda$ , W m<sup>-1</sup> K<sup>-1</sup>) divided by volumetric heat capacity ( $C$ , J m<sup>-3</sup> K<sup>-1</sup>) and reflects both the ability of soil to transfer heat and to change temperature when the heat is supplied or dissipated (Fig. 2). The estimate of thermal conductivity ( $\lambda$ ) and volumetric heat capacity  
170 ( $C$ ) can be described by Eqs. (7-11) (Lu et al., 2014):

$$\lambda_j = \lambda_{dry} + \exp(b_1 - \theta_j^{-b_2}) \quad (7)$$

$$\lambda_{dry} = -0.56\phi + 0.51 \quad (8)$$

$$b_1 = 1.97f_{sa} + 1.87\rho_b - 1.36f_{sa}\rho_b - 0.95 \quad (9)$$

$$b_2 = 0.67f_{cl} + 0.24 \quad (10)$$

$$175 \quad C_j = 1.92 \times 10^6 f_m + 2.51 \times 10^6 f_{OM} + 4.18 \times 10^6 \theta_j \quad (11)$$

where  $\lambda_{dry}$  is oven-dried soil thermal conductivity derived from a linear function of soil porosity ( $\emptyset$ , %).

Both  $b_1$  and  $b_2$  are the shape factors of the  $\lambda$  curve that are estimated by soil texture components. Soil

water content is defined as  $\theta_j$  on the  $j^{\text{th}}$  day ( $\text{cm}^3 \text{cm}^{-3}$ ) and was calculated by the soil water balance

model (Chalhoub et al., 2017). Briefly, the iEM02 operates on a daily time step as daily soil moisture is

180 a function of soil moisture storage capacity ( $\theta^*$ , mm), 24-hour precipitation ( $P$ , mm), and Penman-

Monteith reference evapotranspiration ( $ET_0$ , mm) and are estimated by Eqs. (12-15):

$$\theta_r = 0.026 + 0.005f_{cl} + 0.0158f_{OM} \quad (12)$$

$$\beta_{d,j} = 1 - \exp\left(-\frac{6.68\theta_j h}{(\theta_s - \theta_r)h}\right) \quad (13)$$

$$E_j = \begin{cases} P_j + \beta_{d,j}(ET_{0,j} - P_j) & P_j < ET_{0,j} \\ ET_{0,j} & P_j \geq ET_{0,j} \end{cases} \quad (14)$$

$$185 \quad \theta_j h = \begin{cases} \theta_r h & \theta_j h \leq \theta_r h \\ \theta_{j-1} h + (P_{j-1} - E_{j-1}) & \theta_r h < \theta_j h < \theta^* h \\ \theta_s h & \theta_j h \geq \theta^* h \end{cases} \quad (15)$$

where  $\theta_r$  and  $\theta_s$  define residual and saturated volumetric soil water contents ( $\text{cm}^3 \text{cm}^{-3}$ ).  $\theta_s$  is assumed to

be equal to soil porosity while  $\beta_{d,j}$  is a weighting coefficient for the difference between  $ET_0$  (Allen et al.,

1998) and  $P$  on the  $j^{\text{th}}$  day (-). The initial soil water content ( $\theta_{j-1}$ ) is assumed to be equal half of soil

porosity.

190

Climate observation data prior to the year 2015 were selected to calibrate the iEM02 for each station.

For NE, KS, and OK, daily soil temperature observations at each station had at least 10 years in daily

time series for calibrations. Datasets from TX had at least 4 years available for calibrations. Climate

variables used for calibration included air temperature, precipitation, snow depth, and solar radiation

195 daily observations and the site's static soil property. The optimal parameter values for each weather station were estimated when a minimum root mean square (RMSE) between estimated and observed soil temperature was achieved. These parameters for all 87 stations are listed in [Table A3](#) (see the Appendix).

## 200 **2.3 iEM02 evaluation**

In the datasets selected, all 87 station observations were longer than 15 years except for stations located in Texas. The last five-year observations (2015 to 2019) were used to independently conduct model validation for all 87 stations. The metrics used to evaluate model performance were root mean square error (RMSE) and mean absolute error (MAE). Soil temperature modeling improvement was evaluated  
205 by relative RMSE changes  $\left[-\frac{100(RMSE_{improved} - RMSE_{original})}{RMSE_{original}}\right]$  and by intercomparison between the fully complete model and the reduced model.

## **3 Results and discussion**

### **3.1 Improved empirical model (iEM02)**

210 The iEM02 was evaluated from 2015 to 2019 for 87 weather stations. Soil temperature modeling using different soil textures was improved in different ways in the iEM02 model ([Fig. 3](#)). The improvement of soil temperature modeling indicated by relative RMSE changes was different across sites. The weather stations located in NE and KS as well as TX showed less improvement by introducing the air temperature of  $T_{a,j-3}$  compared to OK ([Fig. 3a](#)). The soil types in OK are more clay and silt compared to  
215 NE and KS ([Fig. 1](#)). However, the improvement by using the fictive environmental temperature was

significant in northern areas of NE and KS (sandy soil) but not in the southern area of OK and part of TX (clay and silt soil) (Fig. 3b). Overall, latitude-dominated air temperature should play a role in improving estimated soil temperature. Most of the 87 stations achieved a 15% to 40% improvement in simulated soil temperature by introducing air temperature  $T_{a,j-3}$  and replacing  $T_a$  with  $T_{env}$ . This  
220 improvement was in agreement with a previous study (Dolschak et al., 2015). By incorporating changes in soil moisture and daily snow depth, additional improvements in soil temperature simulation of up to 50% could be achieved (Fig. 3c) compared to the original model EM02. It should be noted that there were fewer stations available in KS and TX compared to NE and OK. Overall, integrating snow cover and soil moisture data in iEM02 improved the simulated soil temperature (Fig. 3). The daily soil  
225 temperature modeling could be further improved if high-resolution (e.g., 30 m and daily) satellite-based soil moisture/snow cover products become available, for example, products based on the SMAP or Sentinel satellites (Das et al., 2019).

### 3.2 iEM02's parameters

230 The parameters described in iEM02 for each weather station are indicative of soil temperature sensitivities for each independent variable in Eq. (2) although strictly speaking, they are not mathematical sensitivities (Fig. 4 & Table A2). For  $T_{env}$ , the current day  $T_{env}$  was the most weighted as expected (Fig. 4a). The parameters of  $T_{env}$  for the prior day 1 to day 3 were relatively weak in terms of absolute magnitudes due to autoregression properties in the soil temperature (Figs. 4b-d). Interestingly,  
235 in the iEM02 model, the prior day 2 was negatively associated with soil temperature (Fig. 4c) which cannot be interpreted by soil physical processes but in a more autoregressive sense in which the soil

temperature signals are superimposed. The periodic property embedded in iEM02 was two low-frequency components (semi-annual and annual signals). Obviously, the annual signal strength indicated by  $\beta_1$  and  $\delta_1$  was one-order stronger than the semi-annual signal strengths in soil temperature (Fig. 4e-h). The result also suggested the strong  $\beta_1$  and  $\delta_1$  spatial contexts of the northern region (e.g., in Nebraska and Kansas) were differently weighted from those in the southern region (e.g., in Oklahoma and Texas). For the snow damping factor, the snow cover had a larger impact on soil temperature in the northern region when compared to the southern region (Fig. 4i). However, the soil damping ratio factor was relatively evenly distributed (Fig. 4j).

RMSE performance is shown in Figure 5 when the iEM02 was a complete model vs. the reduced model iEM02 where one independent variable term from the complete model was removed. When removing any one independent variable, the modeled soil temperature RMSE increased from 110% to 130% (Fig. 5), indicating a 20% rise in RMSE. Specifically, the iEM02 model performance decreased (i.e., RMSE increased from 0.1 to 0.4°C) when the  $\alpha_0$  term was removed (Fig. 5, a-d). Unlike  $\alpha_0$ , removing the  $\beta_1$  term was not as sensitive and gave an increase of 0.1-0.2°C RMSE on average for all states in the region (Fig. 5, e-h). However, it is clear that the iEM02 model was most sensitive to  $\delta_1$ . With the removal of  $\delta_1$  from the complete iEM02 model, the RMSE increased 0.3-0.4°C for all four states (Fig. 5, i-l). Due to the location-dependency of the above coefficients, further spatial interpolation of the iEM02 model would be beneficial to predict soil temperature for irrigated agricultural areas without weather stations in the U.S. Great Plains and to improve water and crop management modeling.

### 3.3 Spatial and temporal modeling performance

A graphical summary of how closely the modeled soil temperature agreed with the observed soil temperature for each weather station is shown in [Figure 6](#). Daily  $T_s$  estimated in the iEM02 model  
260 outperformed that in the original EM02 model for all 87 weather stations. For example, both MAE and RMSE were decreased on average by 0.6°C when the iEM02 model was used to estimate  $T_s$ . Individually, the improved model showed a less than 1.6°C RMSE for any individual station but 16% of the stations had larger than 2°C RMSE in the original EM02. In addition, we compared the performance of iEM02 against a recent energy-balance model ([Chalhoub et al., 2017](#)). Our prediction of  $T_s$  was  
265 improved by 1.2°C RMSE compared to the energy-balance model (not shown).

Spatial distributions of RMSE showed that the majority of weather stations had better performance in Oklahoma with a mean RMSE of 1.9 and 1.1°C for EM02 and iEM02, respectively, whereas Nebraska had a RMSE of 2.1 and 1.3°C for EM02 and iEM02, respectively. The different modeling performance  
270 was associated with the soil heat transport process and how frequent snowfall could be observed in Nebraska and Oklahoma. Similar results were presented in a recent study by [Huang et al. \(2017\)](#). On the other hand, the high quality of weather data from the Oklahoma Mesonet considered to be the "gold standard" for the statewide weather network ([Lin et al., 2016](#)) thus ensured quality of both model calibrations and observed soil temperature in Oklahoma.

275

Seasonal  $T_s$  indicated that iEM02 modeling was mostly improved in the spring season from 2°C to 1.3°C RMSE ([Fig. 7a](#)) but the original model EM02 showed the uncertainty was in good agreement with the performance achieved in [Plauborg \(2002\)](#). All other seasons were improved in similar ways

from 1.8°C to 1.2 or 1.3°C RMSE. The improvement for all seasons could be attributed to introducing  
280 soil diffusivity, which changed with daily soil moisture and snow cover, and this affected the soil  
thermal conductivity (Rankinen et al., 2004; Zhang, 2005). Moreover, although modeling wintertime  
soil temperature improved from 1.8°C to 1.3°C RMSE, which was the same as in the summer (Fig. 7),  
the soil temperature located in more frequent snow-covered states (e.g., Nebraska and Kansas), was  
better improved when  $T_{env}$  and snow depth were introduced into the model. Our findings confirmed  
285 those reported by Rankinen et al. (2004) and Dutta et al. (2018).

Since precipitation gradients exist in the U.S. Great Plains from western to eastern regions (Evelt et al.,  
2020), three subregions were classified for each state as western (100°W towards west), central  
(between 97° and 100°W), and eastern (97°W towards east). Figure 8 displays the time series of EM02  
290 modeled, iEM02 modeled, and observed soil temperatures only covering winter wheat growing seasons  
(October 1 to June 30) for four growing seasons from 2015 to 2019 (validation periods) in Nebraska and  
Kansas. All subregions in Nebraska and Kansas showed improvement when using the iEM02 model  
(Fig. 8). Similarly, the iEM02 improved the RMSE during four growing seasons in Oklahoma and  
Texas (Fig. 9). The EM02 model had the best performance in Oklahoma with a mean RMSE of 1.0°C,  
295 while the mean RMSE in Kansas was 1.4°C in EM02. Soil temperatures estimated by iEM02 had  
approximately a 0.3 to 1.4°C RMSE (Figs. 8 and 9). In addition, larger improvements by iEM02 were  
observed in most subregions during wintertime, which would be beneficial for modeling winter wheat  
yields and potential yields (Persson et al., 2017).

#### 300 **4. Conclusion**

The primary intention of this work was to develop an improved soil temperature model for the U.S. Great Plains that can predict soil temperature by using common weather station variables as inputs. The improved empirical model (iEM02) integrated soil thermal diffusivity and snow cover factors, and they significantly improved the estimate of soil temperature for 87 weather stations in the U.S. Great Plains that were studied. Specifically, after incorporating changes in soil moisture and daily snow depth, the improved model showed a near 50% gain in performance in terms of RMSE decrease compared to the original model. The value of RMSE across 87 stations was 0.6°C lower on average than the original model from 2015 to 2019. We concluded that the iEM02 model can better estimate soil temperature at the surface soil layer where most hydrological and biological processes occur. Both seasonal and spatial improvements made in the improved model demonstrated the robustness of the iEM02 model, suggesting this improved model can provide a reliable simulation of soil temperature to use in modeling hydrological process and crop production in the U.S. Great Plains.



## Appendix

315 **Table1 A1.** Table of symbols and corresponding descriptions used in this paper.

Symbols	Descriptions	Units
$\alpha$	soil surface albedo	(-)
$\alpha_0, \alpha_1, \alpha_2, \alpha_3$	empirical parameters of air temperature to estimate soil temperature	(-)
$\beta$	empirical parameter of air temperature to calculate environmental temperature	(-)
$\beta_1, \beta_2$	empirical parameters of sine wave to estimate soil temperature	(°C)
$\beta_d$	empirical parameter of evapotranspiration for actual evapotranspiration	(-)
$\delta_1, \delta_2$	empirical parameters of cosine wave to estimate soil temperature	(°C)
$\gamma$	offset constant	(°C)
$\lambda$	soil thermal conductivity	(W m <sup>-1</sup> K <sup>-1</sup> )
$\lambda_{dry}$	oven-dried soil thermal conductivity	(W m <sup>-1</sup> K <sup>-1</sup> )
$\emptyset$	soil porosity	(%)
$\omega$	annual frequency ( $2\pi/365$ or $2\pi/366$ in any leap years)	(-)
$\theta, \theta_r, \theta_s$	actual, residual, and saturated soil water content	(m <sup>3</sup> m <sup>-3</sup> )
$\rho_b$	soil bulk density	(g cm <sup>-3</sup> )
$b_1, b_2$	shape factors of soil thermal conductivity curve	(-)
$C$	soil volumetric heat capacity	(J m <sup>-3</sup> K <sup>-1</sup> )
$D_s$	snow depth	(m)
$DR_{eff}$	effective soil damping ratio	(-)
$E, ET_0$	actual and reference evapotranspiration	(mm)
$f_{cl}, f_m, f_{OM}, f_{sa}$	clay, mineral, organic matter, and sand content in the soil profile	(%)
$f_s$	empirical parameters of snow depth	(m <sup>-1</sup> )
$h$	soil depth	(m)
$j$	day of year	(day)
$k_0$	empirical parameter of soil damping ratio	(-)
$k_s$	soil thermal diffusivity	(m <sup>2</sup> s <sup>-1</sup> )
$p$	period of year (365 days or 366 days in any leap year)	days
$P$	precipitation	mm
$R_s$	solar radiation	(MJ m <sup>-2</sup> d <sup>-1</sup> )
$T_a, T_{max}$	mean and maximum air temperature at 2 m height	(°C)
$T_{env}$	fictive environmental temperature	(°C)
$T_s$	bared soil temperature at 0.1 m depth	(°C)
$T_{sfc}$	surface skin temperature	(°C)
RMSE, MAE	root mean square error and mean absolute error	(°C)

**Table A2.** List of datasets used in this study including the data source (Networks), state names (Coverage States), and specific data variables (Variables). Data sources include the Gridded Soil Survey Geographic (gSSURGO), the Automated Weather Data Network – High Plains Regional Climate Center (AWDN), the Oklahoma Mesonet (OK Mesonet), the Soil Climate Analysis Network (SCAN), and the daily Global History Climatology Network (dGHCN). Weather stations from four states were located in the U.S. Great Plains including Nebraska (NE), Kansas (KS), Oklahoma (OK), and Texas (TX). Climate data reports daily maximum ( $T_{max}$ , °C) and minimum air temperature ( $T_{min}$ , °C) at 2 m height, relative humidity ( $RH$ , %), rainfall ( $prcp$ , mm), solar radiation ( $R_s$ , MJ m<sup>-2</sup> day<sup>-1</sup>), wind speed at 2 m ( $WS$ , m s<sup>-1</sup>), and snow depth ( $D_s$ , mm). Soil data consists of the daily bare soil temperature at 10 cm depth ( $T_s$ , °C), albedo of soil surface ( $\alpha$ , -), organic matter content ( $f_{OM}$ , %), bulk density ( $\rho_b$ , g cm<sup>-3</sup>), porosity ( $\emptyset$ , %), sand ( $f_{sa}$ ), silt ( $f_{sl}$ ), and clay ( $f_{cl}$ ) content (%).

<b>Networks</b>	<b>Coverage States</b>	<b>Variables</b>
gSSURGO	NE, KS, OK, TX	$\alpha, f_{OM}, \rho_b, \emptyset, f_{sa}, f_{sl},$ and $f_{cl}$
AWDN	NE and KS	$T_{max}, T_{min}, RH, prcp, R_s, WS,$ and $T_s$
OK Mesonet	OK	$T_{max}, T_{min}, RH, prcp, R_s, WS,$ and $T_s$
SCAN	TX	$T_{max}, T_{min}, RH, prcp, R_s, WS,$ and $T_s$
dGHCN	NE, KS, OK, TX	$D_s$

330

335 **Table A3.** List of model parameters for each weather station in the U.S. Great Plains. The location consists of latitude (Lat) and longitude (Lon). There are 12 parameters in the improved EM model including parameters of air temperature ( $\beta$ , -); parameters for current day to previous three-day of  $T_{env}$ :  $\alpha_0$  (-),  $\alpha_1$  (-),  $\alpha_2$  (-),  $\alpha_3$  (-), and constant offset  $\gamma$  ( $^{\circ}\text{C}$ ); annual and semi-annual waves of sine and cosine functions parameters:  $\beta_1$ ,  $\beta_2$ ,  $\delta_1$ ,  $\delta_2$  ( $^{\circ}\text{C}$ ); parameters for snow depth damping factor ( $f_s$ ,  $\text{m}^{-1}$ ) and the soil damping factor ( $k_0$ , -). The bold font indicates that estimated coefficients are not statistically significant at 95% confidence intervals.

Location		Parameters in iEM02											
Lat	Lon	$\beta$	$\alpha_0$	$\alpha_1$	$\alpha_2$	$\alpha_3$	$\gamma$	$\beta_1$	$\delta_1$	$\beta_2$	$\delta_2$	$f_s$	$k_0$
26.52	-98.06	0.2	0.402	0.132	-0.18	0.237	7.684	-0.895	-2.212	-0.233	-0.171	-0.05	-0.001
29.33	-103.2	0.3	0.517	0.162	-0.22	0.174	6.221	-0.717	-3.852	0.037	-0.398	-0.106	-0.001
30.27	-97.74	0.8	0.247	0.191	0.017	0.1	8.416	-1.373	-3.454	0.03	-0.269	-0.079	-0.001
31.62	-102.8	0.3	0.369	0.193	-0.13	0.165	6.647	-1.195	-4.451	0.127	-0.365	0.093	-0.001
32.75	-97	0.8	0.216	0.217	0.015	0.088	9.768	-1.338	-2.746	-0.048	-0.167	0.001	0.002
33.59	-102.4	0.3	0.359	0.186	-0.161	0.163	5.656	-1.153	-4.435	0.335	-0.314	0.696	-0.064
33.63	-102.8	0.1	0.421	0.087	-0.175	0.228	4.153	-1.366	-4.637	0.201	-0.077	-0.27	-0.047
33.89	-97.27	0.7	0.415	0.196	-0.01	0.054	4.712	-0.732	-4.197	0.18	0.019	1.187	-0.034
33.96	-102.8	0.3	0.411	0.14	-0.13	0.134	4.949	-1.002	-4.61	0.456	-0.256	0.695	0.001
34.03	-95.54	0.8	0.535	0.136	-0.003	0.058	4.076	-1.164	-2.726	0.306	0.065	-2.045	-0.049
34.04	-96.94	0.6	0.475	0.143	-0.054	0.064	5.196	-1.152	-4.172	0.199	0.054	2.23	-0.066
34.17	-97.99	0.7	0.39	0.103	-0.02	0.056	5.867	-1.032	-3.753	0.136	-0.173	0.232	-0.156
34.19	-97.59	0.8	0.407	0.099	0.009	0.043	4.471	-0.809	-3.197	0.085	-0.091	-1.257	-0.194
34.22	-95.25	0.8	0.408	0.154	0.018	0.049	5.564	-1.358	-3.863	0.104	0.168	-4.133	-0.053
34.31	-96	0.8	0.476	0.097	0.001	0.048	5.499	-1.161	-3.493	0.06	0.015	0.133	-0.108
34.31	-94.82	0.9	0.408	0.139	0.025	0.062	5.947	-0.934	-3.235	0.066	0.006	6.601	-0.065

Location		Parameters in iEM02											
lat	lon	$\beta$	$\alpha_0$	$\alpha_1$	$\alpha_2$	$\alpha_3$	$\gamma$	$\beta_1$	$\delta_1$	$\beta_2$	$\delta_2$	$f_s$	$k_0$
34.57	-96.95	0.5	0.451	0.142	-0.083	0.091	6.331	-1.225	-4.095	0.016	0.075	-1.584	-0.079
34.59	-99.34	0.9	0.266	0.158	0.032	0.071	6.781	-1.68	-4.029	0.345	-0.198	3.081	-0.094
34.61	-96.33	0.5	0.502	0.176	-0.081	0.099	4.733	-1.073	-4.454	0.103	-0.234	-4.241	-0.015
34.66	-95.33	0.9	0.466	0.165	0.021	0.06	5.079	-0.917	-3.484	0.13	0.183	-14.03	-0.029
34.69	-99.83	0.7	0.49	0.153	-0.029	0.056	5.682	-1.341	-4.035	0.139	0.121	<b>-0.068</b>	-0.048
34.73	-98.57	0.9	0.338	0.134	0.019	0.055	4.763	-1.015	-3.158	0.18	<b>0.003</b>	1.937	-0.179
34.8	-96.67	0.7	0.454	0.105	-0.02	0.065	5.742	-1.185	-3.628	0.088	<b>-0.056</b>	-1.26	-0.102
34.81	-98.02	0.8	0.328	0.138	<b>0.008</b>	0.053	5.727	-1.1	-3.811	0.124	<b>-0.05</b>	<b>0.761</b>	-0.129
34.88	-95.78	0.8	0.404	0.111	<b>0.005</b>	0.052	4.723	-1.099	-3.134	0.179	<b>0.018</b>	<b>-0.012</b>	-0.2
35.03	-97.91	0.7	0.52	0.141	-0.028	0.052	5.008	-1.008	-3.33	0.136	0.163	0.845	-0.065
35.19	-102.1	0.6	0.239	0.139	-0.014	0.088	5.715	-1.807	-4.526	0.267	-0.208	-0.129	-0.131
35.27	-97.96	0.8	0.381	0.176	<b>0.011</b>	0.055	5.053	-1.161	-3.341	0.22	-0.093	-0.502	-0.101
35.51	-98.78	0.8	0.39	0.17	<b>0.006</b>	0.05	3.781	-0.779	-2.908	0.078	-0.321	4.582	-0.16
35.55	-99.73	0.5	0.533	0.124	-0.09	0.116	4.372	-1.198	-3.711	0.291	<b>-0.041</b>	0.086	-0.062
35.58	-95.91	0.7	0.391	0.152	<b>-0.015</b>	0.05	5.284	-1.013	-4.053	0.128	0.114	1.057	-0.113
35.59	-99.27	0.8	0.467	0.136	<b>0.011</b>	0.056	5.461	-1.244	-3.594	0.182	0.143	1.237	-0.042
35.68	-94.85	0.6	0.446	0.148	-0.049	0.076	4.758	-1.353	-4.102	0.187	0.248	-3.491	-0.059
35.84	-96	0.6	0.341	0.178	-0.026	0.097	6.618	-1.783	-4.72	0.358	-0.191	<b>-1.872</b>	-0.023
35.85	-97.48	0.9	0.333	0.174	0.021	0.066	5.67	-1.493	-3.899	0.143	0.083	0.914	-0.092
35.97	-94.99	0.7	0.45	0.136	<b>-0.016</b>	0.05	5.637	-1.502	-3.517	0.233	0.094	<b>0.225</b>	-0.047
36	-97.05	0.7	0.414	0.114	<b>-0.007</b>	0.038	4.93	-0.909	-3.849	0.154	<b>-0.037</b>	3.355	-0.156
36.03	-96.5	0.7	0.385	0.149	<b>-0.012</b>	0.053	5.87	-1.13	-4.099	0.093	<b>-0.006</b>	2.131	-0.088
36.07	-99.9	0.7	0.354	0.176	<b>-0.002</b>	0.055	5.608	-1.196	-4.61	0.169	-0.252	1.315	-0.075
36.12	-97.1	0.7	0.377	0.172	<b>-0.009</b>	0.056	5.897	-1.314	-4.027	0.162	<b>0.031</b>	2.05	-0.062
36.26	-98.5	0.7	0.429	0.15	-0.021	0.055	4.908	-1.27	-4.183	0.25	0.265	<b>0.169</b>	-0.067
36.41	-97.69	0.6	0.397	0.175	-0.038	0.079	5.029	-1.188	-4.643	0.089	-0.276	1.137	-0.062
36.42	-96.04	0.9	0.36	0.144	0.017	0.048	5.533	-1.159	-3.882	0.118	0.069	3.667	-0.104
36.52	-96.34	0.7	0.308	0.157	<b>-0.005</b>	0.063	5.684	-1.494	-4.43	0.29	0.149	0.563	-0.13
36.6	-101.6	0.7	0.453	0.173	<b>-0.015</b>	0.078	5.052	-1.21	-3.919	0.261	<b>-0.057</b>	1.796	-0.03
36.63	-96.81	0.6	0.545	0.151	-0.08	0.067	4.993	-0.829	-3.553	0.061	<b>0.031</b>	<b>0.66</b>	-0.061
36.69	-102.5	0.7	0.223	0.16	<b>0.008</b>	0.057	5.711	-1.795	-5.263	0.235	-0.155	1.458	-0.125
36.75	-98.36	0.5	0.474	0.152	-0.083	0.082	4.968	-1.198	-4.11	0.191	<b>-0.011</b>	3.696	-0.072
36.75	-97.25	0.7	0.383	0.167	-0.02	0.056	5.197	-1.086	-4.062	0.005	<b>0.001</b>	4.13	-0.083
36.83	-99.64	0.7	0.354	0.189	<b>-0.004</b>	0.074	5.242	-1.28	-4.03	0.204	<b>0.047</b>	<b>0.367</b>	-0.054
36.84	-96.43	0.6	0.382	0.209	-0.028	0.066	5.279	-1.386	-4.9	0.418	-0.258	-7.259	-0.014
36.9	-96.91	0.6	0.374	0.16	-0.031	0.06	5.007	-1.266	-4.123	0.152	<b>0.021</b>	4.473	-0.103
36.91	-95.89	0.6	0.415	0.169	-0.045	0.053	5.844	-1.22	-4.352	0.235	-0.255	6.361	-0.063
37.37	-95.3	0.7	0.373	0.173	<b>-0.016</b>	0.076	4.535	-1.64	-4.396	<b>0.047</b>	<b>-0.009</b>	<b>-0.77</b>	-0.021

Location		Parameters in iEM02											
lat	lon	$\beta$	$\alpha_0$	$\alpha_1$	$\alpha_2$	$\alpha_3$	$\gamma$	$\beta_1$	$\delta_1$	$\beta_2$	$\delta_2$	$f_s$	$k_0$
37.98	-100.8	0.7	0.346	0.185	<b>0.001</b>	0.077	4.153	-1.319	-4.886	0.084	-0.441	1.602	-0.074
38.45	-101.8	0.4	0.297	0.142	-0.073	0.124	5.091	-2.004	-6.426	0.18	-0.585	1.573	-0.038
38.53	-95.25	0.6	0.46	0.176	-0.053	0.071	3.971	-1.302	-3.761	0.128	-0.075	1.529	-0.054
39.07	-95.78	0.6	0.387	0.162	-0.033	0.089	4.229	-1.715	-4.991	<b>0.019</b>	0.126	<b>0.279</b>	-0.048
39.2	-96.6	0.5	0.4	0.163	-0.077	0.107	4.461	-1.724	-4.951	<b>-0.021</b>	0.081	1.77	-0.025
39.38	-101.1	1	0.252	0.188	0.055	0.075	4.641	-1.501	-5.624	0.062	-0.369	1.507	-0.078
39.82	-97.85	0.8	0.437	0.182	<b>0.008</b>	0.058	3.385	-1.482	-4.33	<b>-0.004</b>	-0.109	<b>-0.429</b>	-0.068
40.08	-98.28	0.5	0.44	0.151	-0.076	0.076	4.164	-1.339	-4.958	<b>-0.017</b>	-0.093	7.636	-0.046
40.3	-96.93	0.7	0.381	0.205	<b>-0.014</b>	0.072	3.293	-1.615	-4.407	0.204	0.088	<b>0.342</b>	-0.064
40.32	-99.38	0.6	0.319	0.199	-0.027	0.055	4.414	-1.593	-5.523	0.25	<b>-0.063</b>	6.898	-0.1
40.4	-101.7	0.6	0.364	0.145	-0.031	0.079	3.559	-1.151	-5.266	0.402	-0.162	8.794	-0.12
40.5	-99.37	0.6	0.337	0.202	-0.029	0.08	4.765	-1.676	-5.194	0.307	0.153	2.688	-0.029
40.52	-99.05	0.6	0.379	0.172	-0.031	0.068	3.676	-1.45	-4.852	0.281	<b>-0.026</b>	5.941	-0.086
40.57	-99.7	0.5	0.329	0.18	-0.051	0.085	3.856	-1.901	-5.549	0.302	0.214	9.566	-0.085
40.57	-98.15	0.8	0.28	0.158	<b>0.013</b>	0.056	4.244	-1.671	-4.596	0.205	0.072	<b>0.708</b>	-0.245
40.63	-100.5	0.7	0.36	0.199	<b>-0.015</b>	0.064	3.888	-1.484	-5.794	0.089	-0.136	3.376	-0.054
40.72	-99.02	0.6	0.406	0.195	-0.034	0.076	3.572	-1.456	-5.1	0.205	<b>0.043</b>	<b>0.756</b>	-0.032
40.75	-98.77	0.5	0.437	0.158	-0.075	0.081	3.778	-1.502	-5.411	0.35	0.097	2.179	-0.078
40.82	-96.67	0.6	0.384	0.193	-0.048	0.066	4.302	-1.619	-4.854	0.111	0.079	3.63	-0.102
40.85	-96.62	0.2	0.588	0.032	-0.209	0.173	3.744	-1.616	-4.753	0.141	0.275	11.447	-0.048
40.86	-98.47	0.5	0.521	0.151	-0.089	0.074	2.731	-1.53	-4.791	0.114	0.309	7.99	-0.067
41.15	-96.5	0.7	0.354	0.169	<b>-0.011</b>	0.065	4.615	-1.819	-4.679	0.124	<b>0.05</b>	4.403	-0.07
41.15	-96.42	0.6	0.42	0.172	-0.055	0.071	3.925	-1.883	-5.022	0.105	0.102	3.669	-0.053
41.22	-103	0.7	0.323	0.188	<b>-0.001</b>	0.054	3.392	-1.118	-5.154	0.263	-0.119	10.875	-0.072
41.4	-97.53	0.5	0.489	0.131	-0.082	0.082	3.624	-1.5	-4.763	0.389	0.074	5.878	-0.057
41.62	-98.95	0.6	0.403	0.164	-0.039	0.077	3.52	-1.649	-5.573	0.136	0.093	2.696	-0.074
41.85	-96.75	0.7	0.336	0.201	-0.025	0.076	4.125	-1.82	-5.053	0.296	0.099	11.111	-0.057
41.88	-103.7	0.7	0.346	0.2	<b>-0.007</b>	0.07	3.58	-1.41	-5.435	0.44	-0.079	4.335	-0.061
41.9	-100.2	0.3	0.548	0.125	-0.195	0.144	2.915	-1.653	-4.817	0.187	0.146	1.078	-0.043
41.93	-98.2	0.5	0.417	0.159	-0.073	0.074	3.353	-1.279	-4.421	0.243	-0.076	10.447	-0.078
42.47	-98.77	0.5	0.509	0.13	-0.104	0.091	3.542	-1.505	-4.489	0.129	0.231	2.505	-0.056
42.57	-99.83	0.3	0.54	0.074	-0.182	0.156	3.049	-1.454	-5.465	0.202	0.286	1.976	-0.077
42.75	-102.2	0.7	0.43	0.144	-0.024	0.068	2.82	-1.142	-5.151	0.141	0.249	3.492	-0.089

## **Code availability**

MATLAB code is available upon request.

## 345 **Data availability**

Data used in this study are available by the links above (material and methods).

## **Author contribution**

350 HZ and XL designed the experiments, conducted simulations, analyzed the data, and wrote the manuscript. NW helped data analysis, result interpretation, and discussion. MBK and GFS provided suggestions and discussion, wrote the manuscripts, and revised the manuscript.

## **Competing interests**

The authors declare that they have no conflict of interest.

355

## **Acknowledgements**

This study was supported in part by the U.S. Department of Agriculture, National Institute of Food and Agriculture (grant no. 2016-68007- 25066 and grant no. 2016-68007- 25066) and the Kansas Crop Improvement Association, the U.S. Department of Agriculture National Institute of Food and  
360 Agriculture, Hatch project 1018005. The contribution number of this manuscript is 20-252-J. We appreciated Dr. Gerard Kluitenberg and Dr. Jesse Tack at Kansas State University for providing helpful suggestions to improve the quality of paper. We thank Dallas Staley for her outstanding contribution in editing and finalizing the paper. Her work continues to be at the highest professional level.

## 365 References

- Abu-Hamdeh, N. H.: Thermal Properties of Soils as affected by Density and Water Content, *Biosystems Engineering*, 86, 97-102, 10.1016/s1537-5110(03)00112-0, 2003.
- Allen, R. G., Pereira, L. S., Raes, D., and Smith, M.: Crop evapotranspiration-Guidelines for computing crop water requirements-FAO Irrigation and drainage paper 56, Fao, Rome, 300, D05109, 1998.
- 405 Araghi, A., Mousavi-Baygi, M., Adamowski, J., Martinez, C., and van der Ploeg, M.: Forecasting soil temperature based on surface air temperature using a wavelet artificial neural network, *Meteorological Applications*, 24, 603-611, 10.1002/met.1661, 2017.
- Badache, M., Eslami-Nejad, P., Ouzzane, M., Aidoun, Z., and Lamarche, L.: A new modeling approach for improved ground temperature profile determination, *Renewable Energy*, 85, 436-444, 10.1016/j.renene.2015.06.020, 2016.
- 410 Badía, D., López-García, S., Martí, C., Ortiz-Perpiñá, O., Girona-García, A., and Casanova-Gascón, J.: Burn effects on soil properties associated to heat transfer under contrasting moisture content, *Science of the Total Environment*, 601, 1119-1128, 2017.
- Bergjord, A. K., Bonesmo, H., and Skjelvåg, A. O.: Modelling the course of frost tolerance in winter wheat, *European Journal of Agronomy*, 28, 321-330, 10.1016/j.eja.2007.10.002, 2008.
- 415 Bittelli, M., Ventura, F., Campbell, G. S., Snyder, R. L., Gallegati, F., and Pisa, P. R.: Coupling of heat, water vapor, and liquid water fluxes to compute evaporation in bare soils, *Journal of Hydrology*, 362, 191-205, 10.1016/j.jhydrol.2008.08.014, 2008.
- Brock, F. V. and Crawford, K. C.: The Oklahoma Mesonet\_ A Technical Overview, *Journal of Atmospheric and Oceanic Technology*, 1995.
- 420 Chalhoub, M., Bernier, M., Coquet, Y., and Philippe, M.: A simple heat and moisture transfer model to predict ground temperature for shallow ground heat exchangers, *Renewable Energy*, 103, 295-307, 10.1016/j.renene.2016.11.027, 2017.
- Das, N. N., Entekhabi, D., Dunbar, R. S., Chaubell, M. J., Colliander, A., Yueh, S., Jagdhuber, T., Chen, F., Crow, W., and O'Neill, P. E.: The SMAP and Copernicus Sentinel 1A/B microwave active-passive high resolution surface soil moisture product, *Remote Sensing of Environment*, 233, 111380, 2019.
- 425 Dhungel, R., Aiken, R., Evett, S. R., Colaizzi, P. D., Marek, G., Moorhead, J. E., Baumhardt, R. L., Brauer, D., Kutikoff, S., and Lin, X.: Energy Imbalance and Evapotranspiration Hysteresis under an Advective Environment: Evidence from Lysimeter, Eddy Covariance, and Energy Balance Modelling, *Geophysical Research Letters*, e2020GL091203, 2021.
- Dirmeyer, P. A. and Norton, H. E.: Indications of surface and sub-surface hydrologic properties from SMAP soil moisture retrievals, *Hydrology*, 5, 36, 2018.
- 430 Dolschak, K., Gartner, K., and Berger, T. W.: A new approach to predict soil temperature under vegetated surfaces, *Modeling earth systems and environment*, 1, 32, 2015.
- Dutta, B., Grant, B. B., Congreves, K. A., Smith, W. N., Wagner-Riddle, C., VanderZaag, A. C., Tenuta, M., and Desjardins, R. L.: Characterising effects of management practices, snow cover, and soil texture on soil temperature: Model development in DNDC, *Biosystems Engineering*, 168, 54-72, 10.1016/j.biosystemseng.2017.02.001, 2018.
- 435 Evett, S. R., Colaizzi, P. D., Lamm, F. R., O'Shaughnessy, S. A., Heeren, D. M., Trout, T. J., Kranz, W. L., and Lin, X.: Past, present, and future of irrigation on the US Great Plains, *Transactions of the ASABE*, 63, 703-729, 2020.
- Goulden, M., Wofsy, S., Harden, J., Trumbore, S. E., Crill, P., Gower, S., Fries, T., Daube, B., Fan, S.-M., and Sutton, D.: Sensitivity of boreal forest carbon balance to soil thaw, *Science*, 279, 214-217, 1998.
- 440 Gupta, S. C., Radke, J. K., Swan, J. B., and Moncrief, J. F.: Predicting soil temperature under a ridge-furrow system in the U.S. Corn Belt, *Soil& Tillage Research*, 18, 145-165, 1990.
- Haacker, E. M., Cotterman, K. A., Smidt, S. J., Kendall, A. D., and Hyndman, D. W.: Effects of management areas, drought, and commodity prices on groundwater decline patterns across the High Plains Aquifer, *Agricultural Water Management*, 218, 259-273, 2019.
- 445 Hillel, D.: *Environmental soil physics: Fundamentals, applications, and environmental considerations*, Elsevier 1998.
- Huang, Y., Jiang, J., Ma, S., Ricciuto, D., Hanson, P. J., and Luo, Y.: Soil thermal dynamics, snow cover, and frozen depth under five temperature treatments in an ombrotrophic bog: Constrained forecast with data assimilation, *Journal of Geophysical Research: Biogeosciences*, 122, 2046-2063, 10.1002/2016jg003725, 2017.

- 450 Kang, S., Kim, S., Oh, S., and Lee, D.: Predicting spatial and temporal patterns of soil temperature based on topography, surface cover and air temperature, *Forest Ecology and Management*, 136, 173-184, 2000.
- Kutikoff, S., Lin, X., Evett, S. R., Gowda, P., Brauer, D., Moorhead, J., Marek, G., Colaizzi, P., Aiken, R., and Xu, L.: Water vapor density and turbulent fluxes from three generations of infrared gas analyzers, *Atmospheric Measurement Techniques*, 14, 1253-1266, 2021.
- 455 Lakshmi, V., Jackson, T. J., and Zehrhuhs, D.: Soil moisture-temperature relationships: results from two field experiments, *Hydrological processes*, 17, 3041-3057, 2003.
- Lembrechts, J. J., Aalto, J., Ashcroft, M. B., De Frenne, P., Kopecky, M., Lenoir, J., Luoto, M., Maclean, I. M. D., Rouspard, O., Fuentes-Lillo, E., Garcia, R. A., Pellissier, L., Pitteloud, C., Alatalo, J. M., Smith, S. W., Bjork, R. G., Muffler, L., Ratier Backes, A., Cesarz, S., Gottschall, F., Okello, J., Urban, J., Plichta, R., Svatek, M., Phartyal, S. S., Wipf, S., Eisenhauer, N., Puscas, M., Turtureanu, P. D., Varlagin, A., Dimarco, R. D., Jump, A. S., Randall, K., 460 Dorrepaal, E., Larson, K., Walz, J., Vitale, L., Svoboda, M., Finger Higgins, R., Halbritter, A. H., Curasi, S. R., Klupar, I., Koontz, A., Pearse, W. D., Simpson, E., Stemkovski, M., Jessen Graae, B., Vedel Sorensen, M., Hoye, T. T., Fernandez Calzado, M. R., Lorite, J., Carbognani, M., Tomaselli, M., Forte, T. G. W., Petraglia, A., Haesen, S., Somers, B., Van Meerbeek, K., Bjorkman, M. P., Hylander, K., Merinero, S., Gharun, M., Buchmann, N., Dolezal, J., Matula, R., Thomas, A. D., Bailey, J. J., Ghosn, D., Kazakis, G., de Pablo, M. A., Kemppinen, J., Niittynen, P., Rew, L., Seipel, T., 465 Larson, C., Speed, J. D. M., Ardo, J., Cannone, N., Guglielmin, M., Malfasi, F., Bader, M. Y., Canessa, R., Stanisci, A., Kreyling, J., Schmeddes, J., Teuber, L., Aschero, V., Ciliak, M., Malis, F., De Smedt, P., Govaert, S., Meeussen, C., Vangansbeke, P., Gigauri, K., Lamprecht, A., Pauli, H., Steinbauer, K., Winkler, M., Ueyama, M., Nunez, M. A., Ursu, T. M., Haider, S., Wedegartner, R. E. M., Smiljanic, M., Trouillier, M., Wilmking, M., Altman, J., Bruna, J., Hederova, L., Macek, M., Man, M., Wild, J., Vittoz, P., Partel, M., Barancok, P., Kanka, R., Kollar, J., Palaj, A., Barros, A., 470 Mazzolari, A. C., Bauters, M., Boeckx, P., Benito Alonso, J. L., Zong, S., Di Cecco, V., Sitkova, Z., Tielborger, K., van den Brink, L., Weigel, R., Homeier, J., Dahlberg, C. J., Medinets, S., Medinets, V., De Boeck, H. J., Portillo-Estrada, M., Verryckt, L. T., Milbau, A., Daskalova, G. N., Thomas, H. J. D., Myers-Smith, I. H., Blonder, B., Stephan, J. G., Descombes, P., Zellweger, F., Frei, E. R., Heinesch, B., Andrews, C., Dick, J., Siebicke, L., Rocha, A., Senior, R. A., Rixen, C., Jimenez, J. J., Boike, J., Pauchard, A., Scholten, T., Scheffers, B., Klinges, D., Basham, E. W., Zhang, J., 475 Zhang, Z., Geron, C., Fazlioglu, F., Candan, O., Sallo Bravo, J., Hrbacek, F., Laska, K., Cremonese, E., Haase, P., Moyano, F. E., Rossi, C., and Nijs, I.: SoilTemp: A global database of near-surface temperature, *Glob Chang Biol*, 10.1111/gcb.15123, 2020.
- Liang, L. L., Riveros-Iregui, D. A., Emanuel, R. E., and McGlynn, B. L.: A simple framework to estimate distributed soil temperature from discrete air temperature measurements in data-scarce regions, *Journal of Geophysical Research: Atmospheres*, 119, 407-417, 10.1002/2013jd020597, 2014.
- 480 Lin, X., Pielke Sr, R. A., Mahmood, R., Fiebrich, C. A., and Aiken, R.: Observational evidence of temperature trends at two levels in the surface layer, *Atmospheric Chemistry and Physics*, 16, 827-841, 10.5194/acp-16-827-2016, 2016.
- Lin, X., Harrington, J., Ciampitti, I., Gowda, P., Brown, D., and Kisekka, I.: Kansas trends and changes in temperature, precipitation, drought, and frost-free days from the 1890s to 2015, *Journal of Contemporary Water Research & Education*, 162, 18-30, 2017.
- 485 Lu, Y., Lu, S., Horton, R., and Ren, T.: An Empirical Model for Estimating Soil Thermal Conductivity from Texture, Water Content, and Bulk Density, *Soil Science Society of America Journal*, 78, 1859-1868, 10.2136/sssaj2014.05.0218, 2014.
- Menne, M. J., Williams Jr, C. N., and Vose, R. S.: The US Historical Climatology Network monthly temperature data, version 2, *Bulletin of the American Meteorological Society*, 90, 993-1008, 2009.
- 490 Meyer, N., Welp, G., and Amelung, W.: The temperature sensitivity (Q10) of soil respiration: controlling factors and spatial prediction at regional scale based on environmental soil classes, *Global Biogeochemical Cycles*, 32, 306-323, 2018.
- Mihalakakou, G., Santamouris, M., Lewis, J., and Asimakopoulos, D.: On the application of the energy balance equation to predict ground temperature profiles, *Solar Energy*, 60, 181-190, 1997.
- Miller, K., Luck, J., Heeren, D. M., Lo, T., Martin, D., and Barker, J.: A geospatial variable rate irrigation control scenario evaluation methodology based on mining root zone available water capacity, *Precision agriculture*, 19, 666-683, 2018.
- 495 Nagare, R. M., Schincariol, R. A., Quinton, W. L., and Hayashi, M.: Effects of freezing on soil temperature, freezing front propagation and moisture redistribution in peat: laboratory investigations, *Hydrology and Earth System Sciences*, 16, 501-515, 2012.



- Nobel, P. S. and Geller, G. N.: Temperature modelling of wet and dry desert soils, *The Journal of Ecology*, 247-258, 1987.
- 500 Onwuka, B. and Mang, B.: Effects of soil temperature on some soil properties and plant growth, *Adv. Plants Agric. Res*, 8, 34-37, 2018.
- Paulsen, G. M. and Heyne, E. G.: Grain production of winter wheat after spring freeze injury, *Agronomy Journal*, 75, 1983.
- Persson, T. and Wirén, A.: Nitrogen mineralization and potential nitrification at different depths in acid forest soils, in: *Nutrient uptake and cycling in forest ecosystems*, Springer, 55-65, 1995.
- 505 Persson, T., Bergjord Olsen, A. K., Nkurunziza, L., Sindhøj, E., and Eckersten, H.: Estimation of Crown Temperature of Winter Wheat and the Effect on Simulation of Frost Tolerance, *Journal of Agronomy and Crop Science*, 203, 161-176, 10.1111/jac.12187, 2017.
- Plauborg, F.: Simple model for 10 cm soil temperature in different soils with short grass, *European Journal of Agronomy*, 17, 173-179, 2002.
- 510 Qi, J., Zhang, X., and Cosh, M. H.: Modeling soil temperature in a temperate region: A comparison between empirical and physically based methods in SWAT, *Ecological Engineering*, 129, 134-143, 2019.
- Qi, J., Li, S., Li, Q., Xing, Z., Bourque, C. P.-A., and Meng, F.-R.: A new soil-temperature module for SWAT application in regions with seasonal snow cover, *Journal of Hydrology*, 538, 863-877, 2016.
- Rankinen, K., Karvonen, T., and Butterfield, D.: A simple model for predicting soil temperature in snow-covered and seasonally frozen soil: model description and testing, *Hydrology and Earth System Sciences*, 8, 706-716, 10.5194/hess-8-706-2004, 2004.
- 515 Rosenberg, N. J., Blad, B. L., and Verma, S. B.: *Microclimate: the biological environment*, John Wiley & Sons 1983.
- Smith, K. A.: *Soil and environmental analysis: physical methods*, revised, and expanded, CRC Press 2000.
- Soong, J. L., Phillips, C. L., Ledna, C., Koven, C. D., and Torn, M. S.: CMIP5 models predict rapid and deep soil warming over the 21st century, *Journal of Geophysical Research: Biogeosciences*, 125, e2019JG005266, 2020.
- 520 Stone, P., Sorensen, I., and Jamieson, P.: Effect of soil temperature on phenology, canopy development, biomass and yield of maize in a cool-temperate climate, *Field crops research*, 63, 169-178, 1999.
- Tack, J., Barkley, A., and Nalley, L. L.: Effect of warming temperatures on US wheat yields, *Proc Natl Acad Sci U S A*, 112, 6931-6936, 10.1073/pnas.1415181112, 2015.
- 525 Williams, J., Jones, C., and Dyke, P. T.: A modeling approach to determining the relationship between erosion and soil productivity, *Transactions of the ASAE*, 27, 129-0144, 1984.
- Williams, J. R., Jones, C. A., Kiniry, J. R., and Spanel, D. A.: The EPIC Crop Growth Model, *Transactions of the American Society of Agricultural Engineers*, 32, 497-511, 1989.
- Wu, S. and Jansson, P.-E.: Modelling soil temperature and moisture and corresponding seasonality of photosynthesis and transpiration in a boreal spruce ecosystem, *Hydrology & Earth System Sciences*, 17, 2013.
- 530 Yan, Q., Duan, Z., Mao, J., Li, X., and Dong, F.: Effects of root-zone temperature and N, P, and K supplies on nutrient uptake of cucumber (*Cucumis sativus* L.) seedlings in hydroponics, *Soil Science and Plant Nutrition*, 58, 707-717, 10.1080/00380768.2012.733925, 2012.
- Yener, D., Ozgener, O., and Ozgener, L.: Prediction of soil temperatures for shallow geothermal applications in Turkey, *Renewable and Sustainable Energy Reviews*, 70, 71-77, 10.1016/j.rser.2016.11.065, 2017.
- 535 Zhang, T.: Influence of the seasonal snow cover on the ground thermal regime: An overview, *Reviews of Geophysics*, 43, 10.1029/2004rg000157, 2005.
- Zhang, T., Shen, S., Cheng, C., Song, C., and Ye, S.: Long-Range Correlation Analysis of Soil Temperature and Moisture on A'rou Hillside, Babao River Basin, *Journal of Geophysical Research: Atmospheres*, 123, 10.1029/2018jd029094, 2018.
- 540 Zhang, Y., Wang, S., Barr, A. G., and Black, T.: Impact of snow cover on soil temperature and its simulation in a boreal aspen forest, *Cold Regions Science and Technology*, 52, 355-370, 2008.
- Zheng, D., Hunt Jr, E. R., and Running, S. W.: A daily soil temperature model based on air temperature and precipitation for continental applications, *Climate Research*, 2, 183-191, 1993.

545

## Figure Captions (9 Figures)

**Figure 1:** Specific soil textures (a) and soil bulk density (b) at 87 weather stations in the U.S. winter wheat belt including the states of Nebraska (NE), Kansas (KS), Oklahoma (OK), and part of Texas (TX) in the U.S. Great Plains.

550 **Figure 2:** Effects of soil moisture on (a) thermal conductivity ( $\lambda$ ) and (b) soil thermal diffusivity ( $k$ ) obtained by Eqs. (7-11).

**Figure 3:** Percentage increments of soil temperature modeling improvement in iEM02 as determined by RMSE changes  $\left[-\frac{100(RMSE_{improved} - RMSE_{original})}{RMSE_{original}}\right]$  (a) after introducing air temperature of  $T_{a,j-3}$ , (b) after substituting air temperature  $T_a$  by fictive environmental temperature ( $T_{env}$ ), and (c) after integrating the impacts of soil thermal diffusivity and snow cover. The colorbar was coded by the improved percentage of iEM02 against the EM02 model.

555

**Figure 4:** Spatial variations of the improved empirical model (iEM) coefficients: (a-d) for  $\alpha_0$ ,  $\alpha_1$ ,  $\alpha_2$ , and  $\alpha_3$ , (e-h) for  $\beta_1$ ,  $\delta_1$ ,  $\beta_2$ , and  $\delta_2$ , (i) snow damping ratio ( $f_s$ ) and (j) soil damping ratio coefficients ( $k_0$ ). The colorbar defines the values of the model's coefficients.

560 **Figure 5:** One-to-one plots of absolute mean errors between the complete model and reduced model where one independent variable term was removed in the improved empirical model (iEM02): (a-d) with vs. without  $\alpha_0$  in Nebraska (NE), Kansas (KS), Oklahoma (OK), and Texas (TX), respectively, (e-h) with vs. without  $\beta_1$  in Nebraska (NE), Kansas (KS), Oklahoma (OK), and Texas (TX), respectively; (i-l) with vs. without  $\delta_1$  in NE, KS, OK, and TX, respectively. The ratio of the root mean square error (RMSE) shown includes both RMSE values calculated from complete and reduced models,

565 respectively. The colorbar indicates the number of observed data points.

**Figure 6:** Spatial distribution of mean absolute error (MAE) (a, c) and RMSE (b, d) for an empirical model (EM02, a, b), and improved model iEM02 (iEM02, c, d). The colorbar defines values of MAE ( $^{\circ}\text{C}$ ) and RMSE ( $^{\circ}\text{C}$ ).

570 **Figure 7:** Seasonal comparison between estimated and observed soil temperatures: (a-d) the empirical model (EM), and (e-h) the improved empirical model (iEM02). RMSE was calculated as the root mean square error between estimated and observed soil temperature. "N" refers to the sample size and the gray line represents the 1:1 line. The colorbar describes the number of data points.

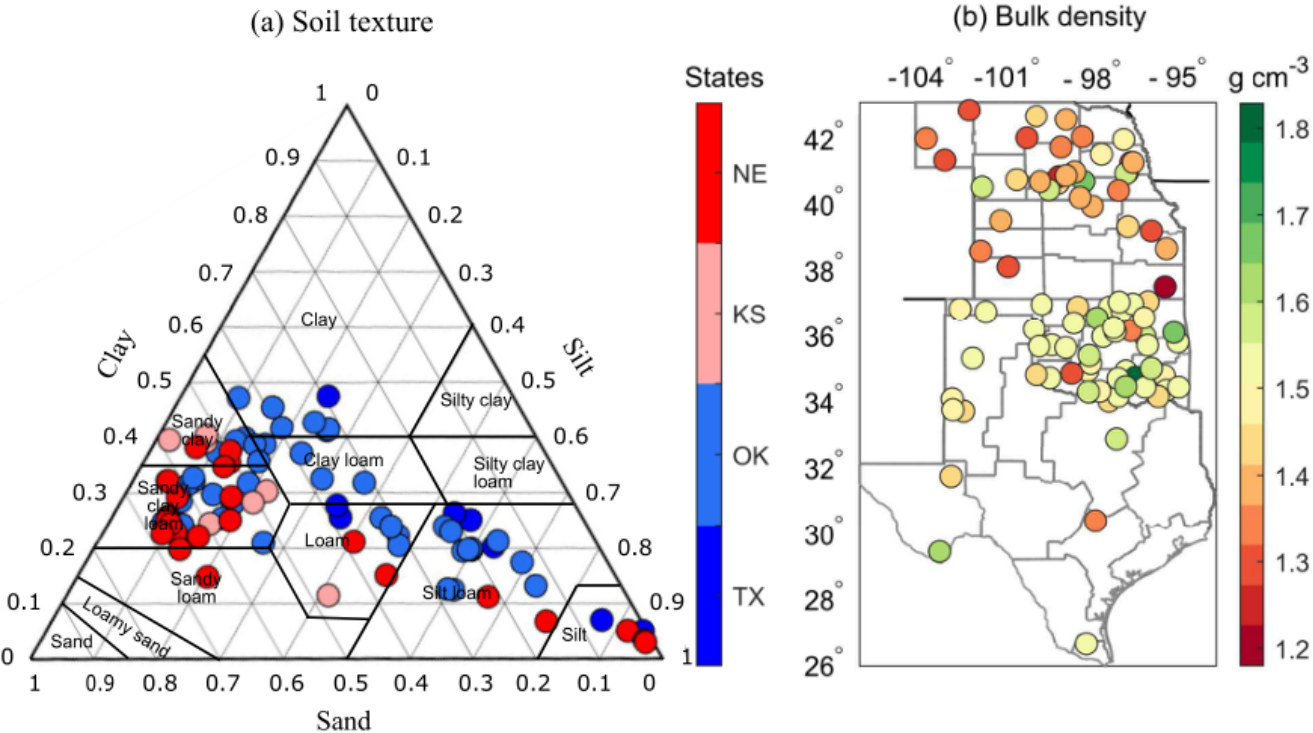
**Figure 8:** Daily soil temperature comparison between observed (grey line), original model (EM02, green line), and improved model (iEM02, blue line) in western ( $>100^{\circ}\text{W}$ ), central (between  $97^{\circ}$  and  $100^{\circ}\text{W}$ ), and eastern ( $<97^{\circ}\text{W}$ ) Nebraska (a-c) and Kansas (d-f) during the winter wheat growing seasons from 2015 to 2019. RMSE is the root mean square error ( $^{\circ}\text{C}$ ). The values in brackets refer to both RMSE values of original model (green numbers) and improved model (blue numbers) during the

575

580 periods of October-November, December-January-February, and March-April-May-June, respectively.  
Shaded areas highlight the winter season (December-February).

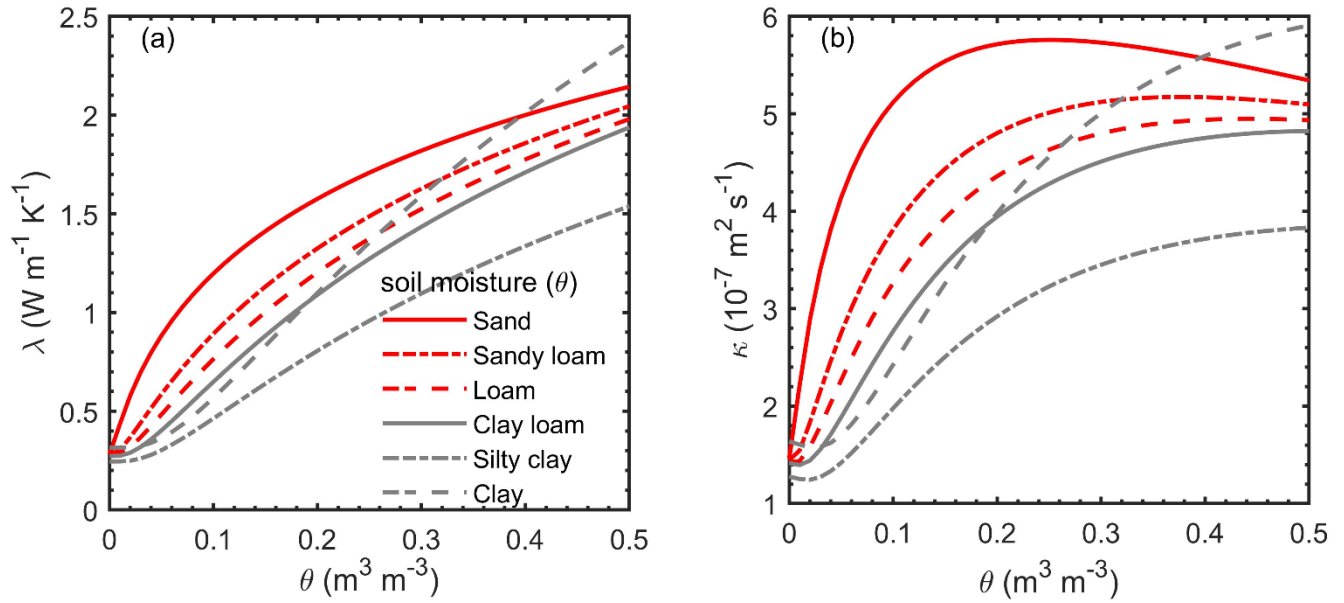
**Figure 9:** The same as Fig. 8 but for western, central, and eastern Oklahoma (**a-c**) and Texas (**d-f**).

Figure 1.



585 **Figure 1:** Specific soil textures (a) and soil bulk density (b) at 87 weather stations in the U.S. winter wheat belt including the states of Nebraska (NE), Kansas (KS), Oklahoma (OK), and part of Texas (TX) in the U.S. Great Plains.

**Figure 2.**



**Figure 2:** Effects of soil moisture on (a) thermal conductivity ( $\lambda$ ) and (b) soil thermal diffusivity ( $k$ ) obtained by Eqs. (7-11).  
590

**Figure 3.**

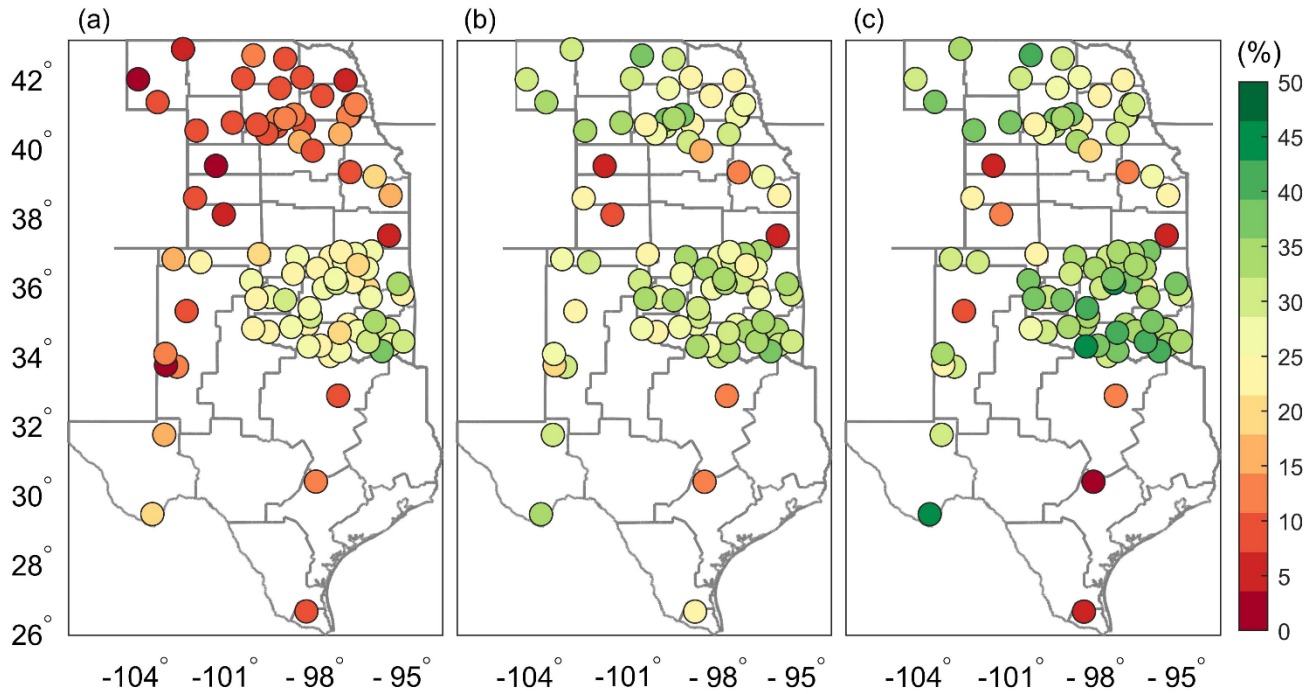
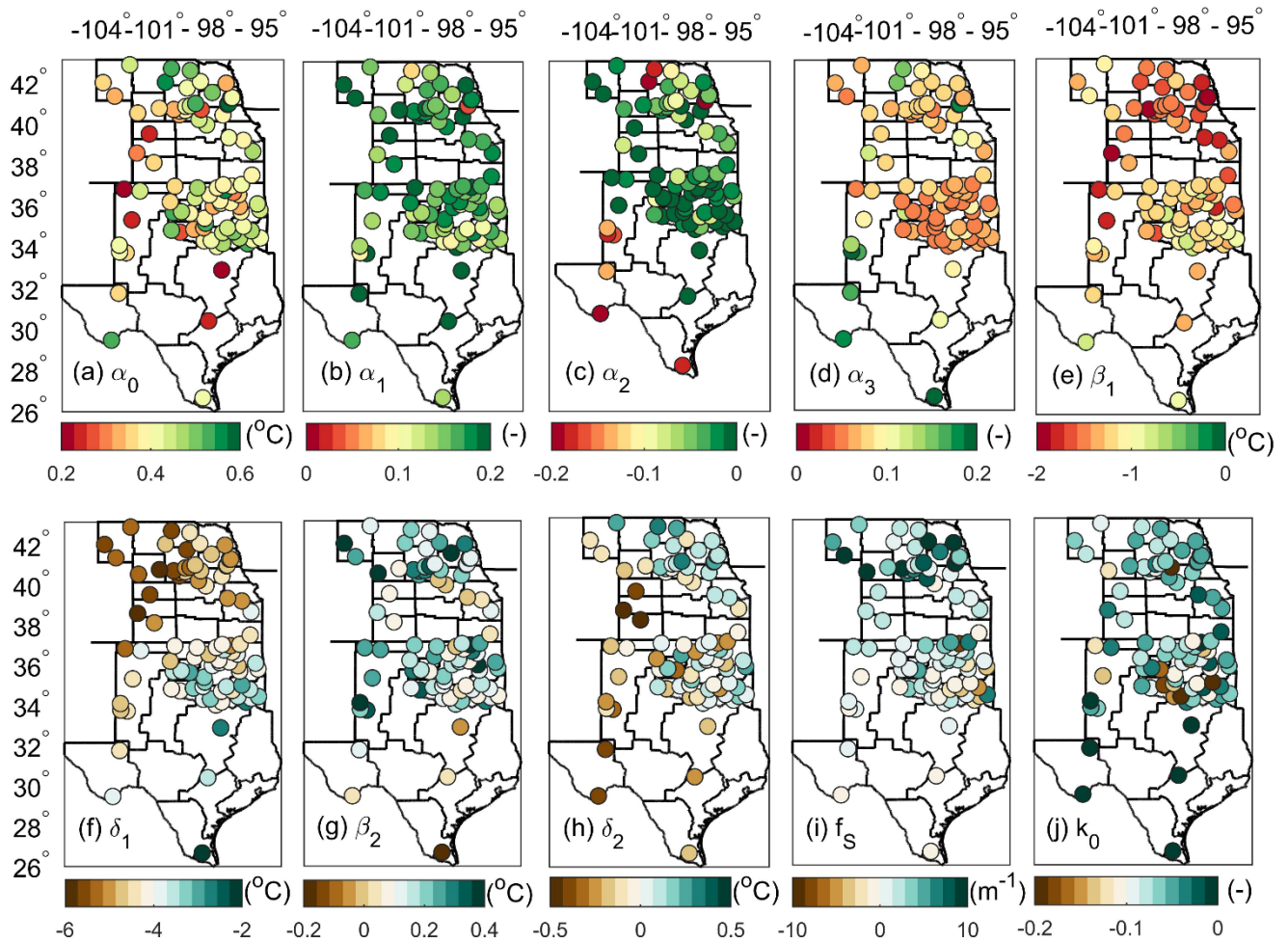


**Figure 3:** Percentage increments of soil temperature modeling improvement in iEM02 as determined by RMSE changes  $\left[-\frac{100(RMSE_{improved} - RMSE_{original})}{RMSE_{original}}\right]$  (a) after introducing air temperature of  $T_{a,j-3}$ , (b)

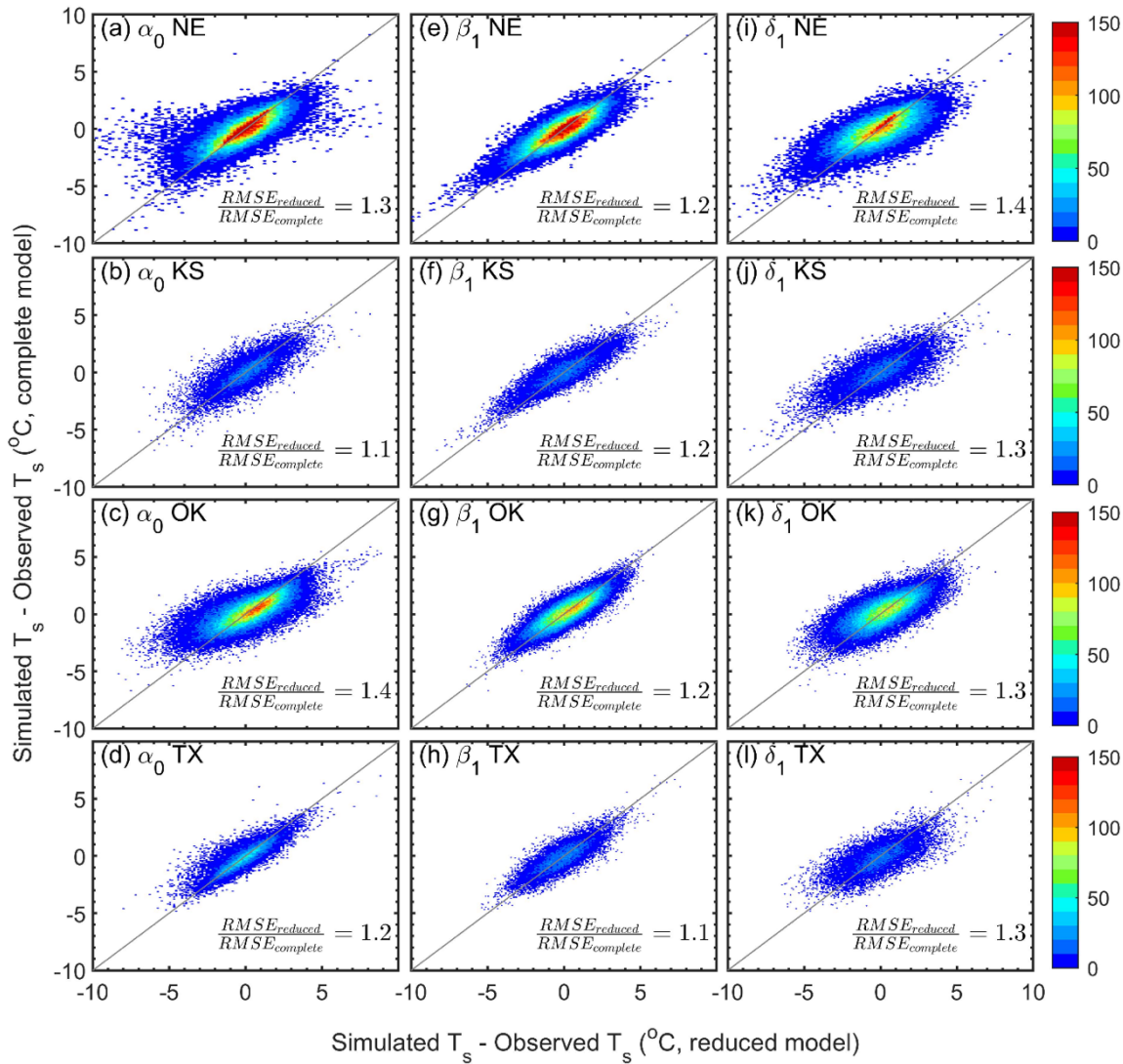
595 after substituting air temperature  $T_a$  by fictive environmental temperature ( $T_{env}$ ), and (c) after integrating the impacts of soil thermal diffusivity and snow cover. The colorbar was coded by the improved percentage of iEM02 against the EM02 model.

**Figure 4.**



600 **Figure 4:** Spatial variations of the improved empirical model (iEM) coefficients: **(a-d)** for  $\alpha_0$ ,  $\alpha_1$ ,  $\alpha_2$ , and  $\alpha_3$ , **(e-h)** for  $\beta_1$ ,  $\delta_1$ ,  $\beta_2$ , and  $\delta_2$ , **(i)** snow damping ratio ( $f_s$ ) and **(j)** soil damping ratio coefficients ( $k_0$ ). The colorbar defines the values of the model's coefficients.

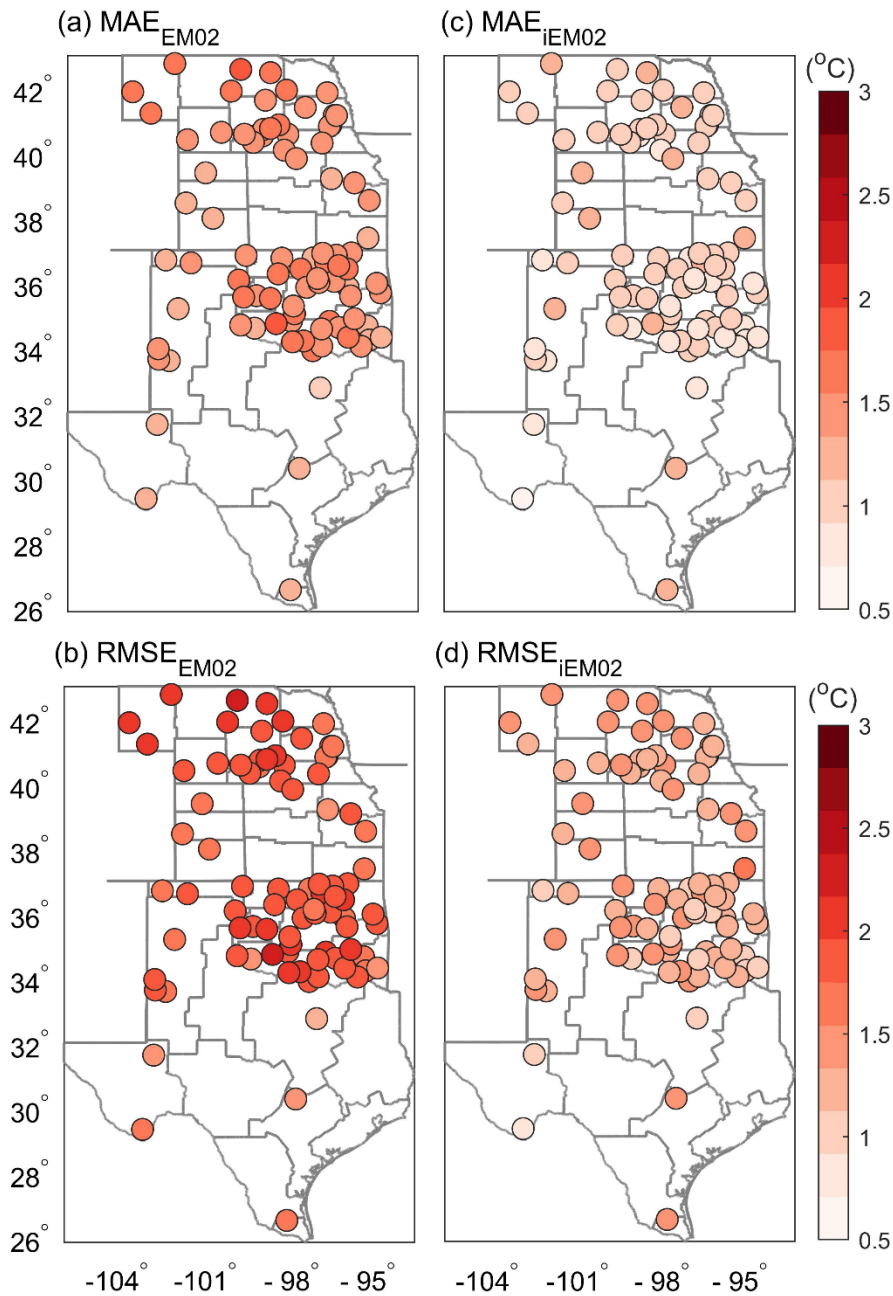
**Figure 5.**



605 **Figure 5:** One-to-one plots of absolute mean errors between the complete model and reduced model  
 where one independent variable term was removed in the improved empirical model (iEM02): **(a-d)**  
 with vs. without  $\alpha_0$  in Nebraska (NE), Kansas (KS), Oklahoma (OK), and Texas (TX), respectively, **(e-**  
**h)** with vs. without  $\beta_1$  in Nebraska (NE), Kansas (KS), Oklahoma (OK), and Texas (TX), respectively;  
**(i-l)** with vs. without  $\delta_1$  in NE, KS, OK, and TX, respectively. The ratio of the root mean square error  
 610 (RMSE) shown includes both RMSE values calculated from complete and reduced models,  
 respectively. The colorbar indicates the number of observed data points.

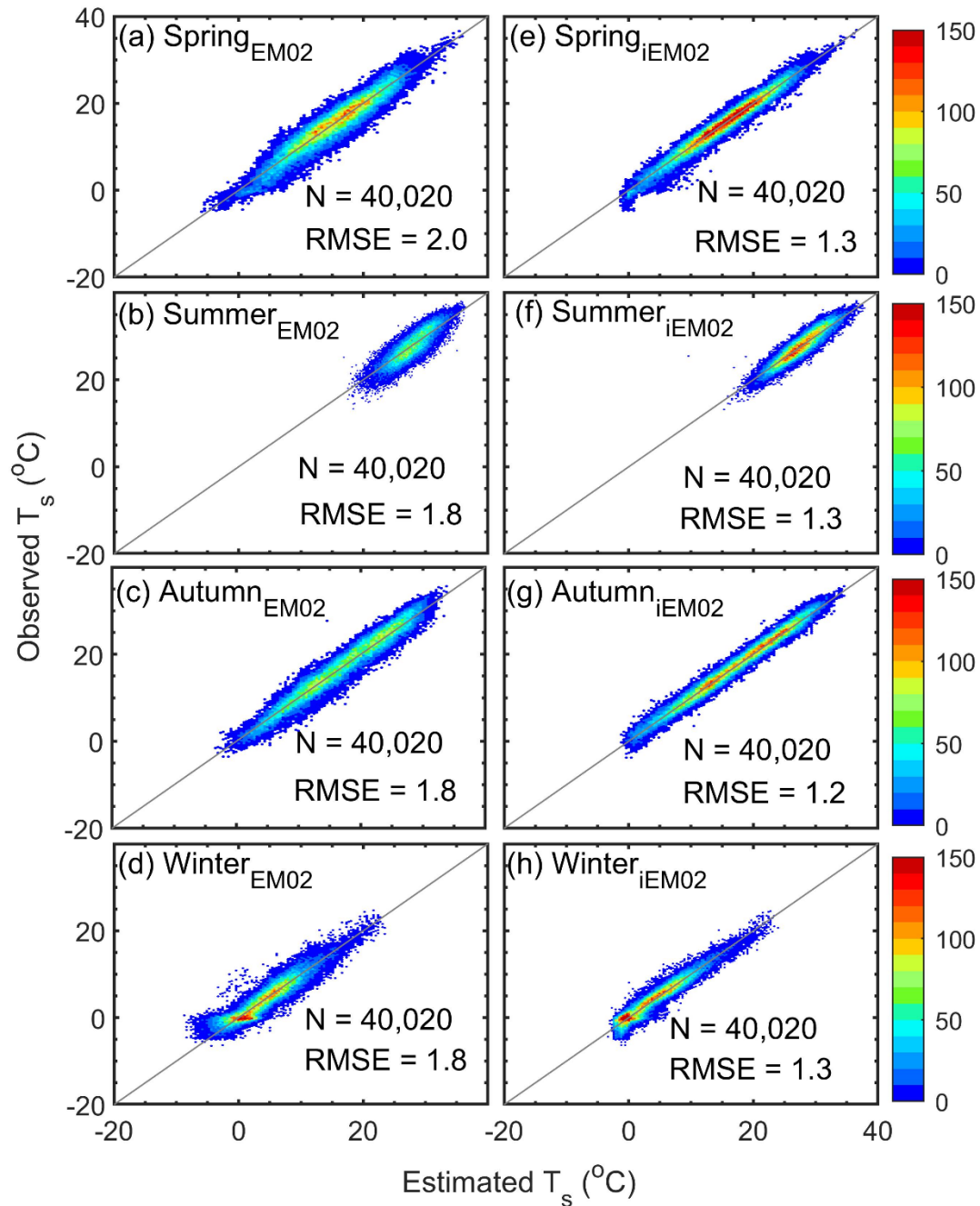


Figure 6.



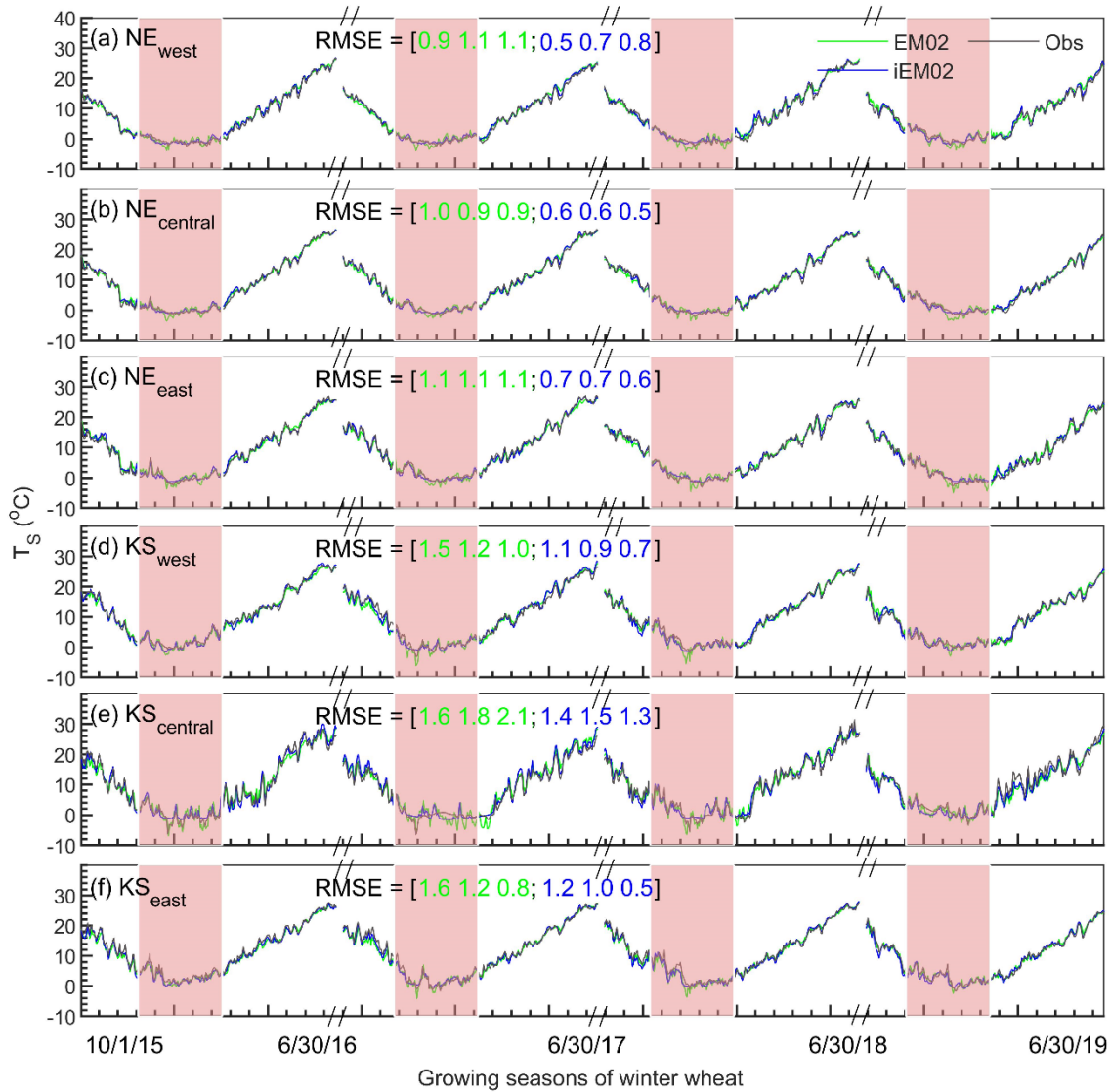
615 **Figure 6:** Spatial distribution of mean absolute error (MAE) (a, c) and RMSE (b, d) for an empirical model (EM02, a, b), and improved model iEM02 (iEM02, c, d). The colorbar defines values of MAE (°C) and RMSE (°C).

Figure 7.

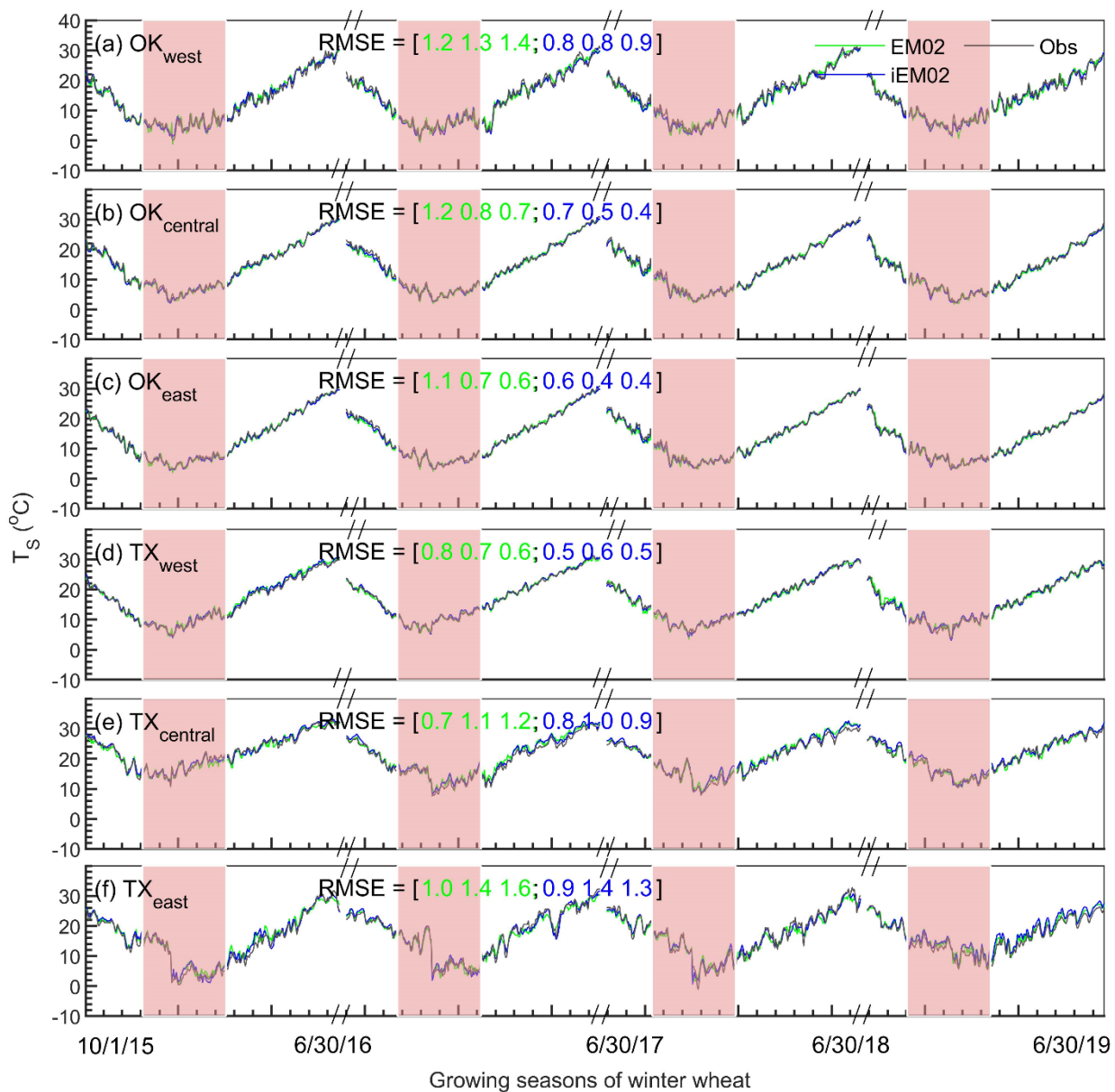


620 **Figure 7:** Seasonal comparison between estimated and observed soil temperatures: (a-d) the empirical model (EM), and (e-h) the improved empirical model (iEM02). RMSE was calculated as the root mean square error between estimated and observed soil temperature. "N" refers to the sample size and the gray line represents the 1:1 line. The colorbar describes the number of data points.

**Figure 8.**



**Figure 8:** Daily soil temperature comparison between observed (grey line), original model (EM02, green line), and improved model (iEM02, blue line) in western ( $>100^{\circ}\text{W}$ ), central (between  $97^{\circ}$  and  $100^{\circ}\text{W}$ ), and eastern ( $<97^{\circ}\text{W}$ ) Nebraska (a-c) and Kansas (d-f) during the winter wheat growing seasons from 2015 to 2019. RMSE is the root mean square error ( $^{\circ}\text{C}$ ). The values in brackets refer to both RMSE values of original model (green numbers) and improved model (blue numbers) during the periods of October-November, December-January-February, and March-April-May-June, respectively. Shaded areas highlight the winter season (December-February).

**Figure 9.****Figure 9:** The same as Fig. 8 but for western, central, and eastern Oklahoma (a-c) and Texas (d-f).